Supporting Information

Solid polymer electrolytes with sacrificial end groups for wide oxidative potential and stable interfaces in lithium metal batteries

*Ashish Raj,[¥] Satyannarayana Panchireddy,[¥] Lieven Bekaert,[α] Bruno Grignard,[Ψ] Christophe Detrembleur,[Ψ] and Jean-François Gohy[¥] **

[¥]Institute of Condensed Matter and Nanoscience (IMCN), UCLouvain, Place L. Pasteur 1, 1348 Louvain-la-Neuve, Belgium

[α]Electrochemical and Surface Engineering (SURF), Department of Materials and Chemistry, Vrije Universiteit Brussel, 1050 Brussels, Belgium

Eenheid Algemene Chemie (ALGC), Vrije Universiteit Brussel (VUB), 1050 Brussels, Belgium

[Ψ]Center for Education and Research on Macromolecules (CERM), CESAM Research Unit, University of Liège, 13 Allée du 6 août, Building B6A, 4000 Liège, Belgium

Federation of Researcher in Innovation Technologies for CO_2 transformation (FRITCO2T research platform), University of Liège, 13 Allée du 6 août, Building B6A, 4000 Liège, Belgium

*Corresponding author: jean-francois.gohy@uclouvain.be

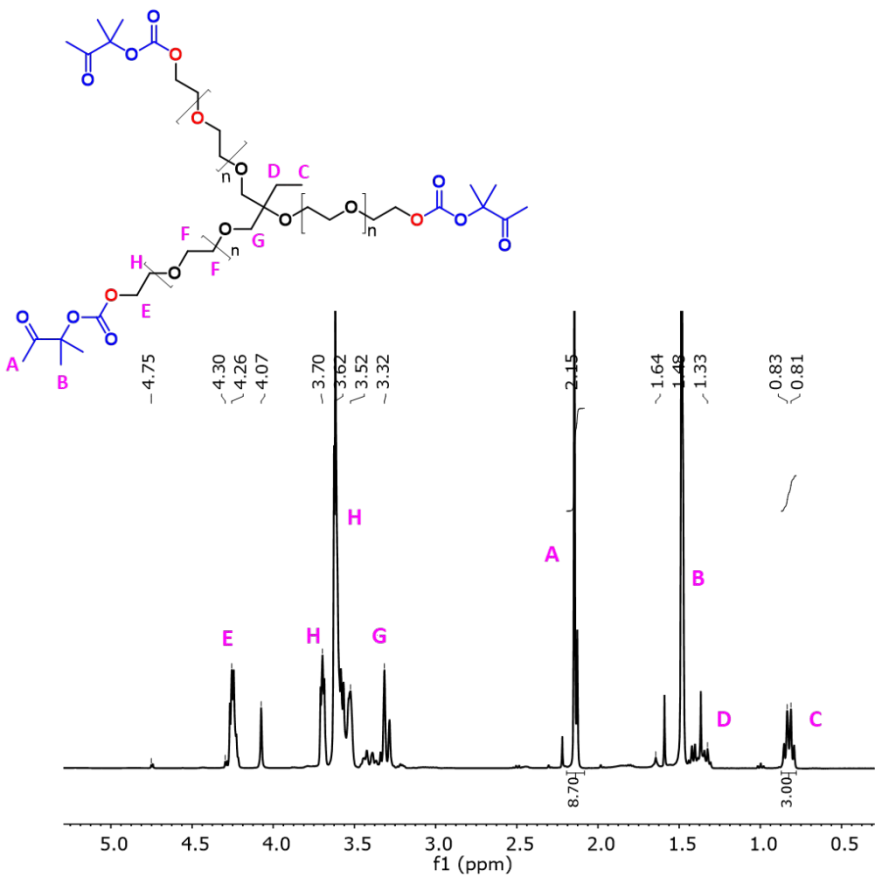

Figure S1. ^{1}H NMR spectra of tri-arm poly(ethylene glycol) carbonate-ketone (TPEG-Carb-ket).

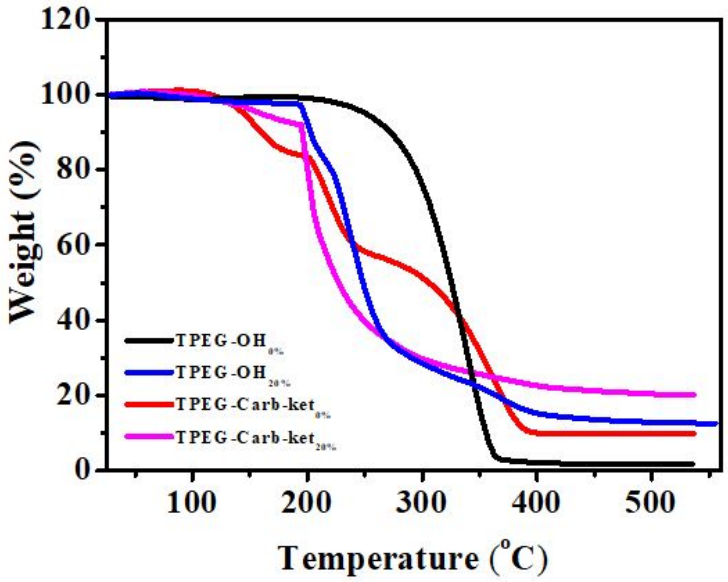

Figure S2. Thermogravimetric analysis of TPEG-OH and TPEG-Carb-ket with and without LiTFSI (wt % indicated in subscript).

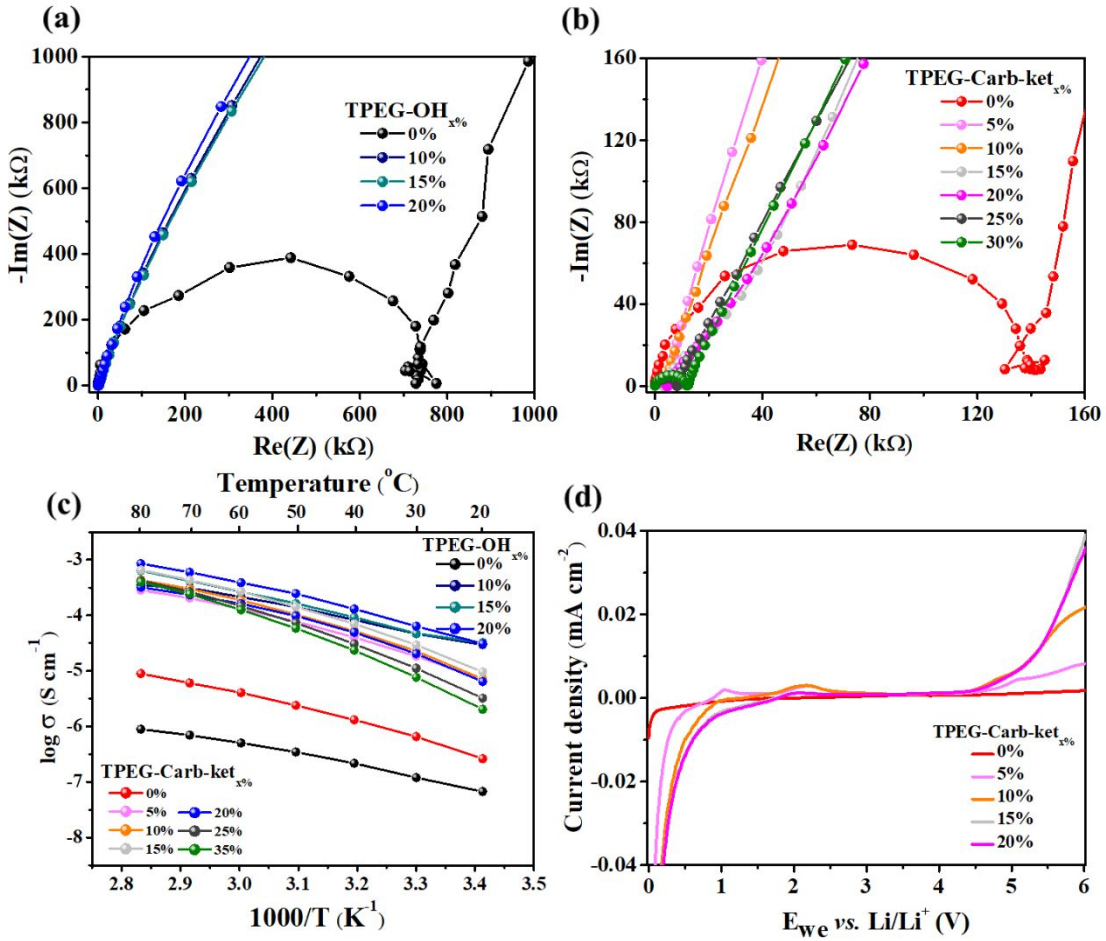

Figure S3. Nyquist plots of a) TPEG-$OH_{x\%}$; b) TPEG-Carb-$ket_{x\%}$ at 30 °C; c) Temperature dependent ionic conductivity for TPEG-$OH_{x\%}$ and TPEG-Carb-$ket_{x\%}$ and d) Linear sweep voltammetry of Li|TPEG-Carb-$ket_{x\%}$|SS at 1 mV s^{-1}, 30 °C (x indicating the wt% of LiTFSI).

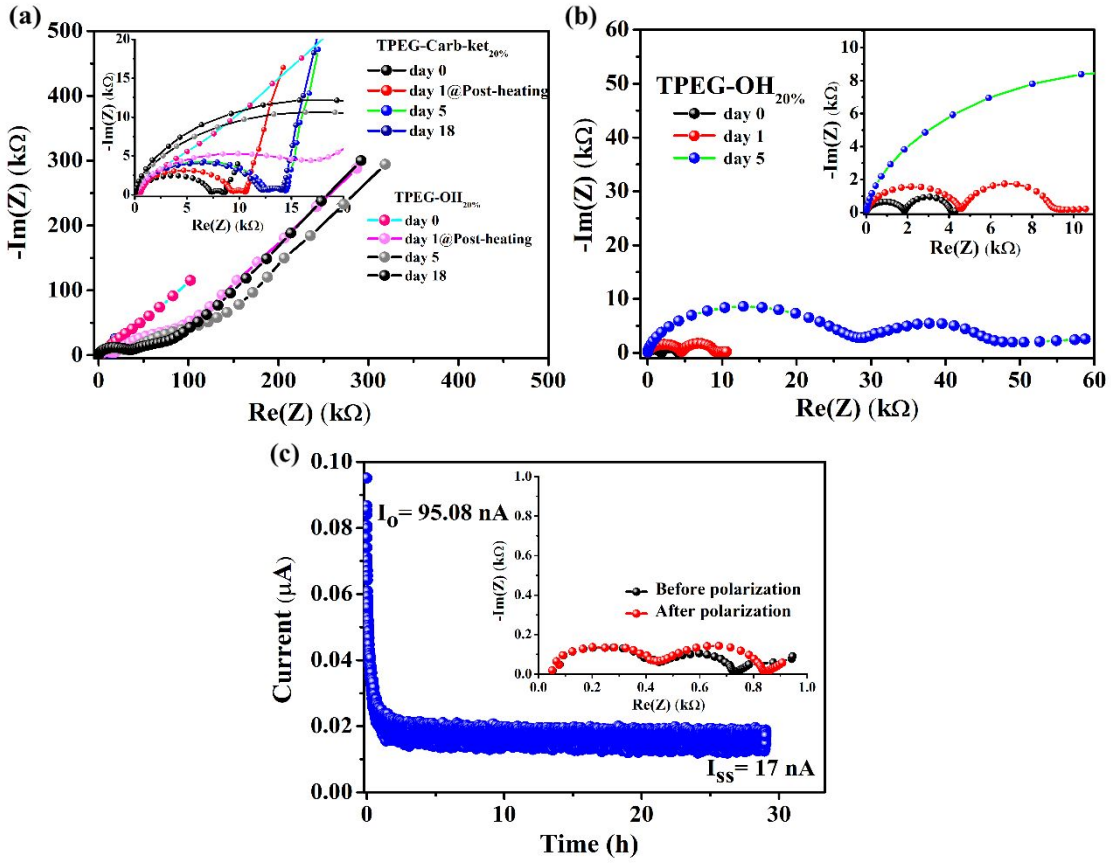

Figure S4. Nyquist plots of a) for Cu|TPEG-$OH_{20\%}$|Li and Cu|TPEG-Carb-$ket_{20\%}$|Li, respectively at open circuit potential and RT; b) for Li|TPEG-$OH_{20\%}$|Li and c) Chronoamperometry and impedance measurement for transference number calculation of Li|TPEG-Carb-$ket_{20\%}$|Li cell.

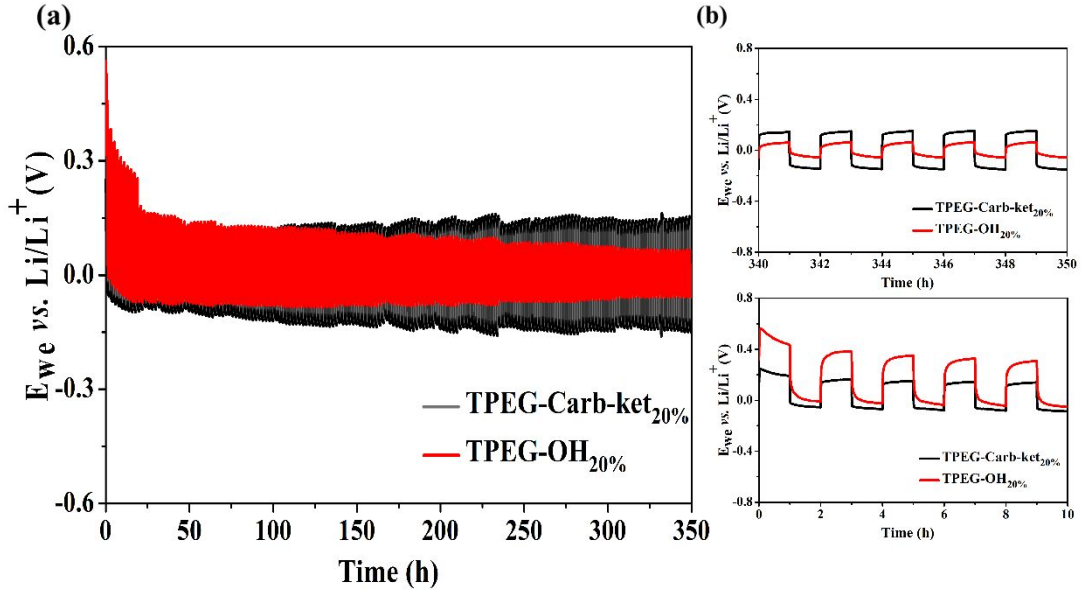

Figure S5. a) Stripping and plating of Lithium for TPEG-OH$_{20\%}$ and TPEG-Carb-ket$_{20\%}$ with Li-Li symmetric cell at RT and b) Enlarged view of a) in 340-350 h and 0 – 10 h, respectively.

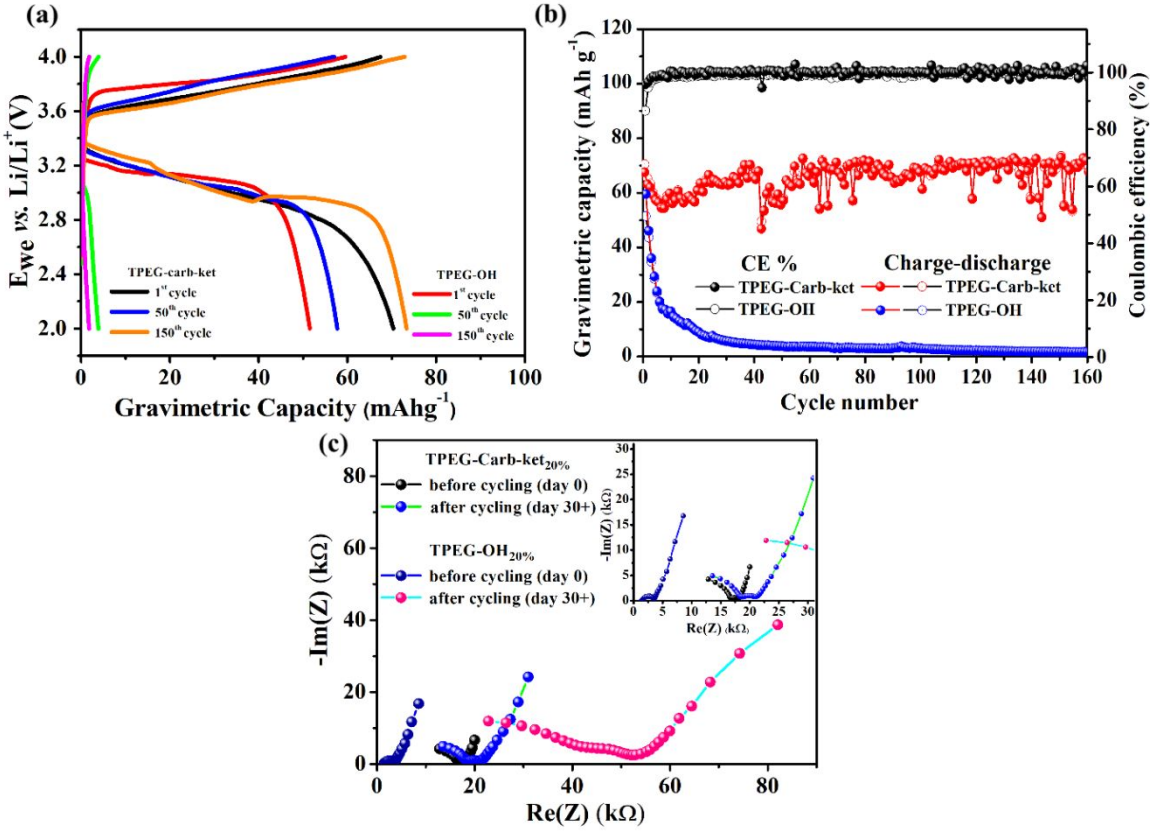

Figure S6. Galvanostatic charge-discharge voltage profile for TPEG-Carb-ket$_{20\%}$ and TPEG-OH$_{20\%}$ with gravimetric capacity; a) At following charge and discharge of specific cycle at 0.1C; b) Capacity retention plot with cycle number for Li|TPEG-Carb-ket$_{20\%}$|LFP and Li|TPEG-OH$_{20\%}$|LFP, respectively at 0.1C and RT; c) Nyquist plot before PEIS before and after cycling of Li|TPEG-OH$_{20\%}$|LFP and Li|TPEG-Carb-ket$_{20\%}$|LFP (magnified scale in inset).

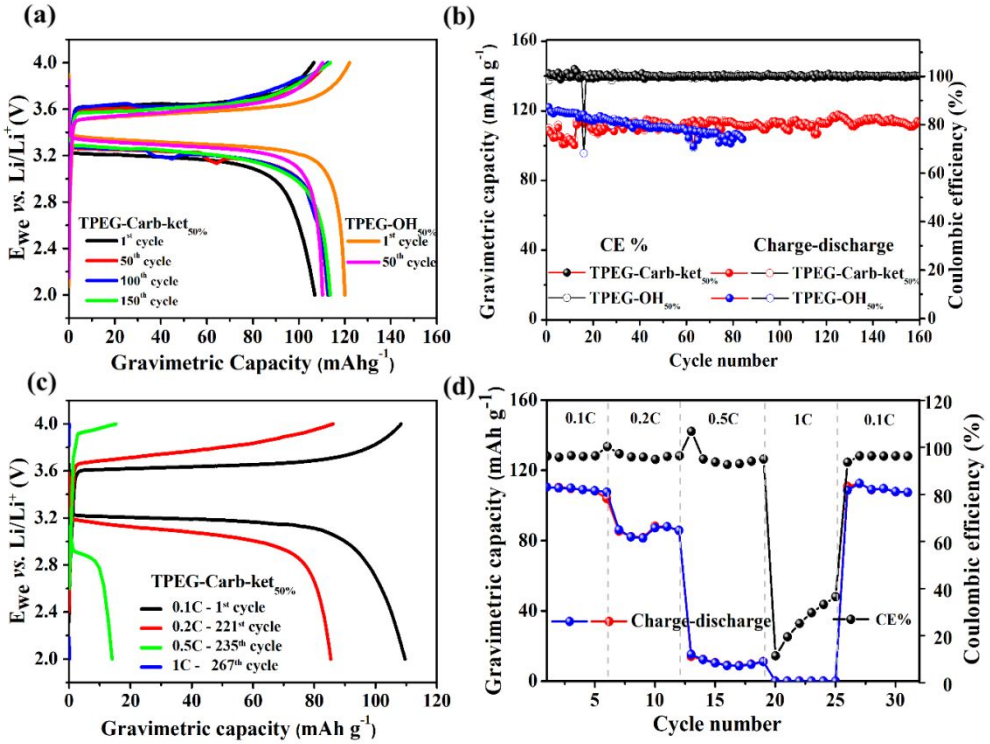

Figure S7. Galvanostatic charge-discharge voltage profile for TPEG-Carb-ket$_{50\%}$ and TPEG-OH$_{50\%}$ with gravimetric capacity; a) At following charge and discharge of specific cycle at 0.1C; b) Capacity retention plot with cycle number for Li|TPEG-Carb-ket$_{50\%}$|LFP and Li|TPEG-OH$_{50\%}$|LFP, respectively at 0.1C and RT; c) Galvanostatic charge-discharge voltage profile at different C-rate; d) Rate capability plot with different C-rate for Li|TPEG-carb-ket$_{50\%}$|LFP.

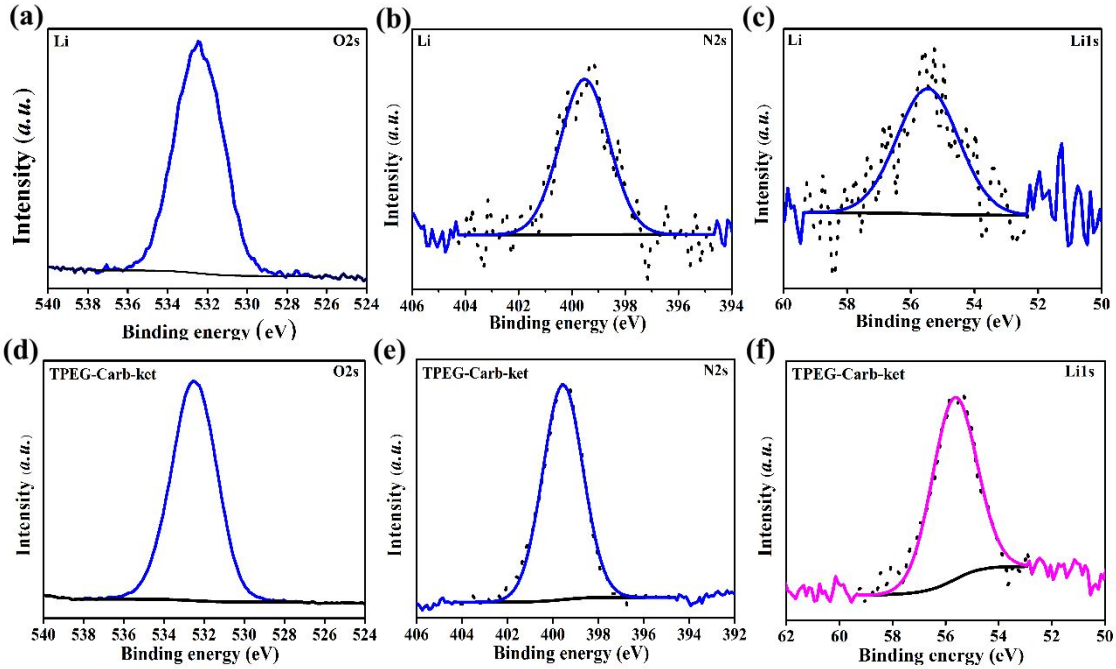

Figure S8. HR-XPS of a) and d) oxygen (O1s), b) and e) nitrogen (N1s), c) and f) lithium (L1s) for lithium metal and TPEG-Carb-ket of cycled Li|TPEG-Carb-ket$_{20\%}$|LFP cell.

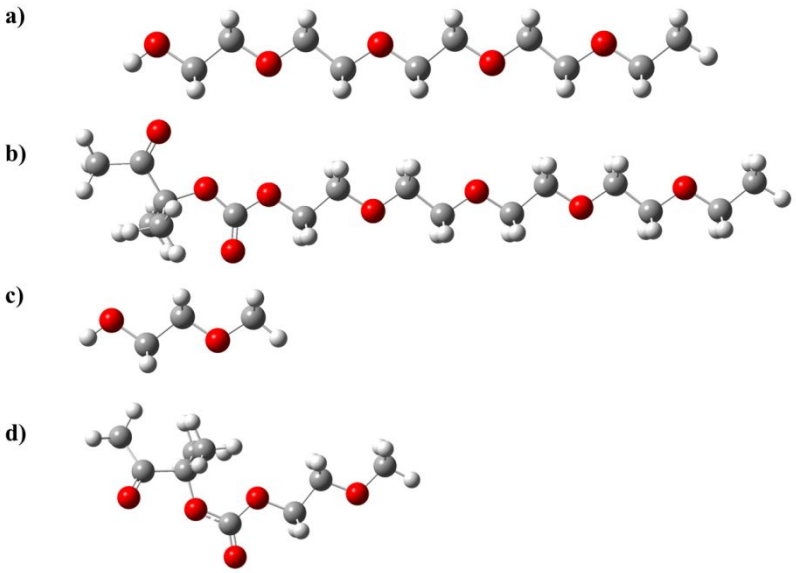

Figure S9. Energy-minimized structures used in the quantum chemical calculations; a) and b) Structures used in HOMO-LUMO orbital calculations, -OH ending and -Carb-ket ending, respectively; c) and d) Structures used in AIMD simulations, -OH ending and -Carb-ket ending, respectively. The size of the structures was reduced in the case of the AIMD simulations to allow for shorter simulation times due to the high computational cost.

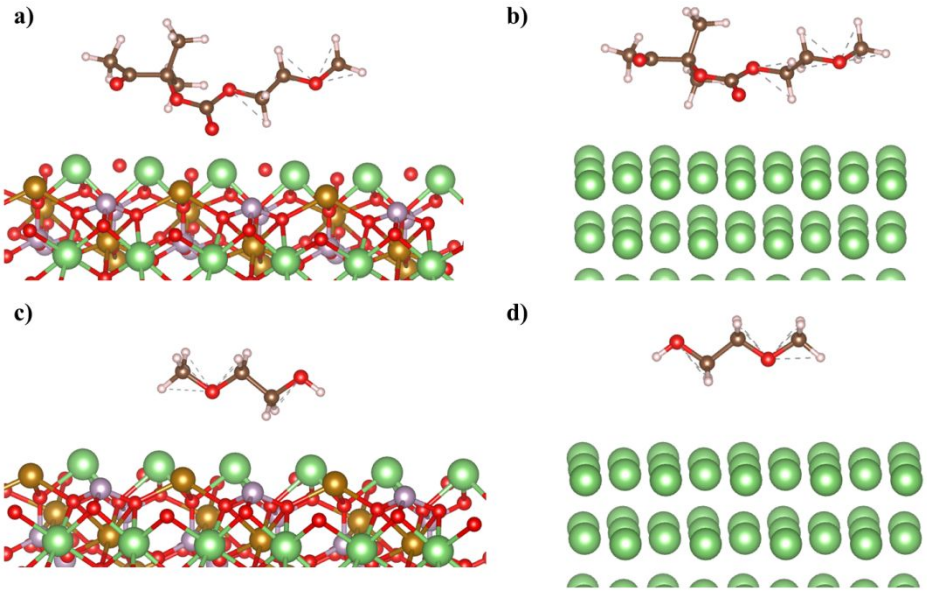

Figure S10. AIMD simulation input structures; a) -Carb-ket ending on LFP b) Carb-ket ending on Li c) -OH ending on LFP d) -OH ending on Li.

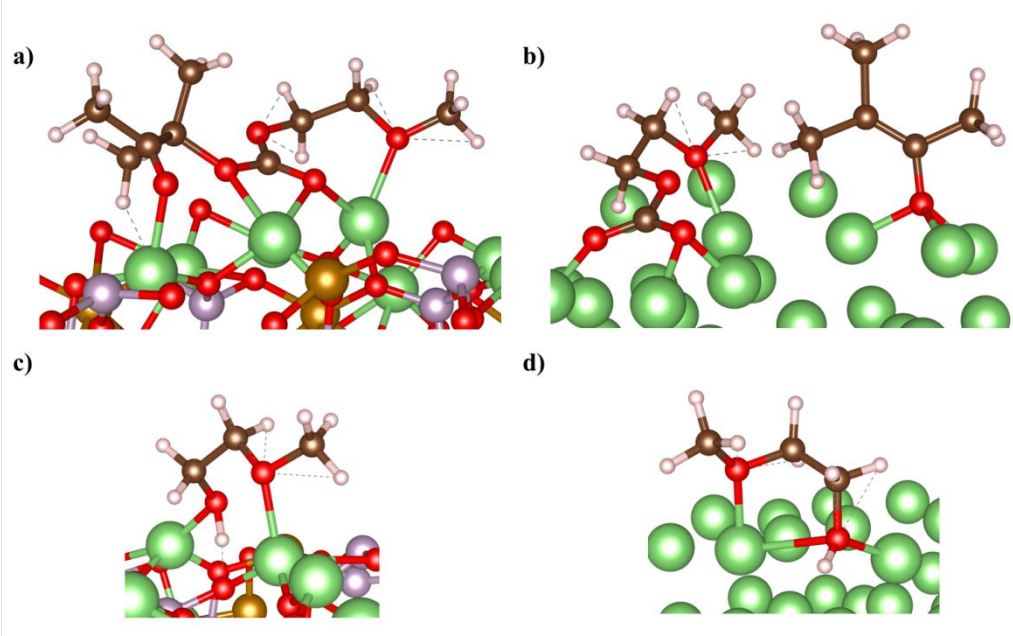

Figure S11. AIMD simulation structures after 5 ps: a) -Carb-ket ending on LFP; b) Carb-ket ending on Li; c) -OH ending on LFP; d) -OH ending on Li. In b) A reaction occurred in which the bond between a tertiary carbon atom and the carbonate group broke.

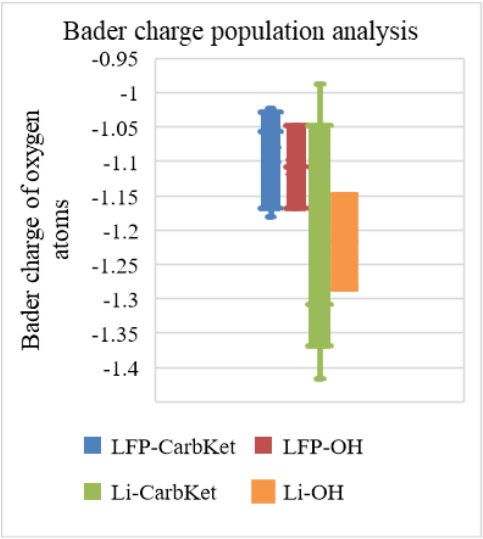

Figure S12. Bader charge population analysis for the oxygen atoms in the terminal groups for the AIMD simulation structures after 5 ps. On the lithium metal electrodes, some of the oxygen atoms had an even more negative charge for the -Carb-ket group as opposed to the -OH group, indicating a greater reactivity.

Table S1: Quantification table of XPS analysis of electrodes post-cycling indicating binding energy (BE), full width half maxima (FWHM) and abundance ratio (%).

		F 1s			O 1s	N 1s			C 1s						S 2p$_{3/2}$	Si 2p	Li 1s
		F-C	F-Li	F total		N-(C,H)$^+$	N-(C,H)	N total	O=C-O, C-F	C=O, O-C-O	C-(O,N)	C-(C,H)	C$_x$	C total	Sulphate	Si	
Li anode	BE	687.5	684.8		532.5		399.5		289.3	287.8	286.3	284.8	282.7		169.6		55.5
	FWHM	2.1	2.1		2.9		2.2		1.7	1.7	1.7	1.7	1.7		1.9		2.3
	A%	3.7	9.4	13.1	28.8		1.2	1.2	1.9	3.5	8.7	33.9	0.6	48.64	1.6		6.7
TPEG-Carbket	BE	687.4	684.5		532.6		399.6		289.8	287.8	286.3	284.8	282.1		169.6	102.1	56.7
	FWHM	2.3	1.8		2.6		2.1		1.6	1.6	1.6	1.6	1.6		1.8	1.9	2.0
	A%	2.2	0.8	2.9	23.5		1.9	1.9	2.5	6.8	13.8	39.9	0.4	63.4	3.2	0.1	3.6